
A Reverse Flow–Metabolism Mismatch Pattern on PET Is Related to Multivessel Disease in Patients with Acute Myocardial Infarction

Hiroyuki Yamagishi, Kaname Akioka, Kumiko Hirata, Yuji Sakanoue, Kazuhide Takeuchi, Junichi Yoshikawa and Hironobu Ochi

First Department of Internal Medicine and Division of Nuclear Medicine, Osaka City University Medical School, Osaka, Japan

Hypoperfused myocardium with increased uptake of ^{18}F -fluorodeoxyglucose (FDG) is considered to be ischemic but viable myocardium. However, the significance of a more severe defect of FDG than of ^{13}N ammonia (NH_3) (i.e., reverse flow–metabolism mismatch) is not well understood. **Methods:** To study a reverse flow–metabolism mismatch pattern, PET with NH_3 and FDG under glucose loading was performed in 35 patients within 2 wk after onset of first acute myocardial infarction (AMI) and in 29 patients with old myocardial infarction (OMI). The left ventricle was divided into nine segments on a bull's eye polar map, and the mean counts of NH_3 (% NH_3) and FDG (%FDG) were compared for the segment with the least % NH_3 . **Results:** Ten patients in the AMI group demonstrated a marked reverse flow–metabolism mismatch pattern (greater than 10% difference between % NH_3 and %FDG), whereas only 2 patients in the OMI group demonstrated the mismatch pattern ($P < 0.05$). Sixteen patients with AMI demonstrated %FDG $>$ % NH_3 (group 1), and 19 patients with AMI demonstrated %FDG $<$ % NH_3 (group 2). There were no significant differences in age, sex, location of infarction, diameter of stenosis of infarct-related artery or left ventricular ejection fraction between groups 1 and 2. Eleven patients in group 2 and only 3 in group 1 had multivessel disease ($P < 0.02$). There was no significant relationship between the number of diseased vessels and the flow–metabolism pattern in patients with OMI. **Conclusion:** The finding of a reverse flow–metabolism mismatch on PET in the subacute phase of myocardial infarction was closely related to multivessel disease.

Key Words: PET; myocardial infarction; multivessel disease

J Nucl Med 1999; 40:1492–1498

Glucose, lactate and free fatty acids are the major sources of energy for the heart. In the fasting state, the myocardium mainly uses free fatty acid, whereas in the fed state, glucose becomes more important (1,2). Striking changes occur in substrate utilization during myocardial ischemia. Because β -oxidation of free fatty acids is very sensitive to ischemia, the principal fuel-contributing substrate for the

citric acid cycle during ischemia is glucose (3). Mild to moderate ischemia increases myocardial glucose uptake (4).

PET permits assessment of regional myocardial perfusion and metabolism in vivo. Hypoperfused myocardium with increased uptake of ^{18}F -fluorodeoxyglucose (FDG) as an indicator of exogenous glucose utilization is considered to be ischemic but viable myocardium, with the potential for improvement of regional function after restoration of blood flow (5–10). Although a flow–metabolism mismatch pattern has been shown to be indicative of reversibly dysfunctional myocardium in patients with chronic coronary artery disease (5–10), this marker has not been as reliable for patients with recent myocardial infarctions (11–13).

In the course of our experience with ^{13}N -ammonia (NH_3)–FDG PET, patients with myocardial infarctions occasionally were noted to have more severe defects of FDG than of NH_3 (i.e., a reverse flow–metabolism mismatch pattern). In most previous reports, more severe defects of FDG than of NH_3 were included in a flow–metabolism mismatch pattern. No study examining the significance of reverse flow–metabolism mismatch phenomenon is available. To study this phenomenon, NH_3 and glucose-loaded FDG PET studies, therefore, were performed in patients with myocardial infarctions.

MATERIALS AND METHODS

Patients

Thirty-five patients suffering their first acute myocardial infarctions (AMIs) (29 men, 6 women; mean age 64 ± 10 y; range 40–79 y) and 29 patients with documented previous, old myocardial infarction (OMI) (25 men, 4 women; mean age 65 ± 6 y; range 50–76 y) underwent myocardial perfusion and metabolism studies with PET. AMI diagnosis was based on the presence of typical and prolonged chest pain, ST-segment elevation or depression on standard 12-lead electrocardiograms and elevation of serum creatine kinase to more than three times the normal upper limit. Patients who had undergone previous coronary angioplasty of arteries other than the infarct-related artery or coronary artery bypass grafting were excluded from this study. Patients who had suffered more than two myocardial infarctions were excluded from the group of patients with OMI.

Of the 35 patients with AMI, 17 had anterior infarctions and 18

Received Sep. 24, 1998; revision accepted Feb. 4, 1999.
For correspondence or reprints contact: Hiroyuki Yamagishi, MD, First Department of Internal Medicine, Osaka City University Medical School, 1–5–7 Asahi-Machi, Abeno-Ku, Osaka 545–8586, Japan.

had inferior infarctions (including one inferolateral infarction). Of the 29 patients with OMI, 21 had suffered anterior infarctions and 8 had suffered inferior infarctions. No patient had a pure lateral infarction. All patients with AMI underwent PET using FDG and NH₃ within 2 wk (range 6–14 d, mean 10 ± 3 d) after the onset of myocardial infarction. For patients with OMI, the interval between the onset of infarction and the PET study was 33 ± 52 mo (range 2–168 mo).

Radiopharmaceuticals

A small cyclotron (NKK Corporation, Kanagawa, Japan) was used for the production of ¹³N and ¹⁸F. NH₃ was then produced using the method described by Mulholland et al. (14), and FDG was synthesized using the method described by Hamacher et al. (15).

PET Imaging

For PET imaging, a Shimadzu-SET 1400 W-10 PET scanner (HEADTOME IV; Shimadzu Corp., Kyoto, Japan) was used. This scanner can obtain 7 slices simultaneously with a 13-mm interval, a slice thickness of 11-mm full width at half maximum (FWHM) and spatial resolution of 4.5-mm FWHM. Axial, 6.5-mm-interval Z-motion of the scanner provided a total of 14 contiguous transverse slices of the myocardium.

A 10-min transmission scan was obtained using a rotating ⁶⁸Ge rod source. The acquired data were used to correct emission images of NH₃ and FDG for body attenuation. After completion of the transmission scan, the patient remained in the supine position and was injected intravenously with 555–740 MBq NH₃. After a 3-min delay to allow pulmonary background activity to clear, myocardial perfusion imaging was performed for 10 min.

Three to 4 h after completion of the perfusion scan, FDG PET imaging was performed postprandially. Identical patient positioning for the NH₃ and FDG images was achieved by marking the subject's chest wall with ink and aligning the marks with a reference beam of light from the gantry. The patient was injected intravenously with 259–370 MBq FDG 30–60 min after the patient ate his or her usual meal, supplemented with a 50-g glucose solution. Forty to 50 min were allowed for cardiac uptake of FDG. Static imaging of glucose utilization was then performed for 10 min. In this study, 13 patients had diabetes mellitus: 6 patients were treated with diet only, 3 with oral hypoglycemic agents and 4 with insulin. The treatment for their diabetes mellitus was not withheld during the studies, and no additional treatment was given in glucose loading for FDG PET imaging.

Images were collected in 256×256 matrices and reconstructed by a computer system (Dr. View; Asahi-Kasei Joho System Co., Ltd., Tokyo, Japan) using Butterworth and ramp filters along the short axis of the heart.

Quantitative Analysis of PET Images

Each short-axis slice was divided into 36 sectors, 10° each, and a bull's eye polar map was reconstructed from the short-axis slices extending from the base to the apex. The maximal count in the left ventricle was selected, and the value of each pixel was normalized to a maximal count of 100. The left ventricle was divided into nine segments as shown in Figure 1, and the mean of normalized counts of each segment was calculated. The mean counts of NH₃ (%NH₃) and FDG (%FDG) were compared for the segment demonstrating the least %NH₃, which was considered to be the center of infarction.

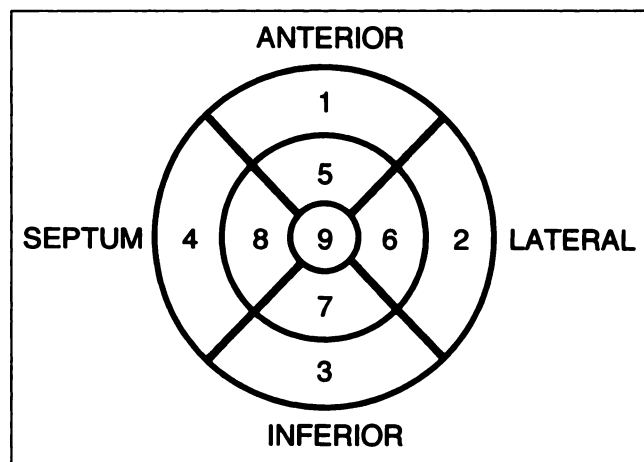


FIGURE 1. Schematic diagram of nine segments of left ventricle on bull's eye polar map.

Coronary Arteriography and Left Ventriculography

Eleven patients with AMI underwent successful coronary angioplasty of the infarct-related artery within 24 h after the onset of myocardial infarction. Twenty-four patients underwent coronary arteriography during the subacute phase (within 6 wk after onset) but had undergone no coronary intervention before the PET studies. All patients with OMI underwent coronary arteriography within 2 wk of PET study. Coronary arteriography was performed in multiple projections using standard techniques. Quantitative coronary narrowing analysis was performed using a computer-assisted, automated edge-detection algorithm (QCA-CMS Cardiovascular Measurement System Ver 3.0; MEDIS Medical Imaging System, Leiden, The Netherlands), and coronary artery narrowing was expressed as the maximal percentage narrowing of luminal diameter. Narrowing exceeding 50% in the major epicardial coronary arteries (right coronary artery 1, 2, 3, main left coronary artery 5, left anterior descending artery 6, 7 and left circumflex 11, 13 in the American Heart Association reporting system [16]) was considered significant. Infarct-related arteries were considered diseased regardless of percentage narrowing of diameter. Left ventriculography was performed in 31 patients with AMI and in all patients with OMI. The ejection fraction of the left ventricle was calculated by the single plane-area length method.

Peak Creatine Kinase

Venous blood samples for estimation of the peak serum creatine kinase were drawn every 3 h for the first 24 h and every 6 h for the next 24–48 h after the onset of infarction. All patients demonstrated significant elevations of serum creatine kinase, but peak values could be determined for only 27 patients with AMI and were documented in only 13 with OMI.

Statistics

Continuous variables were expressed as mean \pm SD. The unpaired *t* test was used to compare continuous variables between two groups. The paired *t* test was used to compare %NH₃ and %FDG. One-way analysis of variance was used to compare continuous variables among four groups. Post hoc comparisons were made by Scheffe's test. Groups were compared for categorical data by the χ^2 test. *P* > 0.05 was considered significant.

RESULTS

As shown in Table 1, there was no significant difference in age, sex, location of infarction, peak creatine kinase, diameter of stenosis of the infarct-related artery, coronary intervention in the infarct-related artery, %NH₃ or %FDG between the AMI and OMI patients. However, the OMI group included more patients with diabetes mellitus, collateral circulation to infarct-related artery, multivessel disease and low left ventricular ejection fraction than the AMI group. The AMI group included 10 patients with a marked reverse flow–metabolism mismatch pattern (>10% difference between %NH₃ and %FDG), whereas the OMI group included only 2 patients with a marked reverse flow–metabolism mismatch pattern ($P < 0.05$).

Of the 35 patients with AMI, 16 had %FDG > %NH₃ in the segment with the least %NH₃ (group 1), and 19 had %FDG < %NH₃ (group 2). Of the 29 patients with OMI, 16 had %FDG > %NH₃ in the segment with the least %NH₃ (group 3), and 13 had %FDG < %NH₃ (group 4).

The differences between %NH₃ and %FDG (%FDG – %NH₃) were $9\% \pm 7\%$ (range 0%–26%) in group 1, $-12\% \pm 9\%$ (range -2% to -34%) in group 2, $9\% \pm 6\%$ (range 0%–19%) in group 3 and $-6\% \pm 4\%$ (range -1% to

-17%) in group 4. The %FDG-to-%NH₃ ratios were 1.22 ± 0.23 (range 1.00–1.84) in group 1, 0.78 ± 0.13 (range 0.45–0.95) in group 2, 1.23 ± 0.18 (range 1.00–1.62) in group 3 and 0.85 ± 0.08 (range 0.74–0.99) in group 4.

Baseline Characteristics and PET Data for Acute Myocardial Infarction Patients

As shown in Table 1, there were no significant differences in age, sex, location of infarction, diabetes mellitus, peak creatine kinase, stenosis diameter of the infarct-related artery, collateral circulation, coronary intervention to the infarct-related artery or left ventricular ejection fraction between groups 1 and 2. However, group 2 included more patients with multivessel disease ($P < 0.02$). There was no significant difference in %NH₃ between the two groups, whereas %FDG was smaller in group 2 than in group 1 ($P < 0.003$).

Baseline Characteristics and PET Data for Old Myocardial Infarction Patients

As shown in Table 1, there were no significant differences in age, sex, location of infarction, diabetes mellitus, peak creatine kinase, stenosis diameter of the infarct-related artery, collateral circulation, coronary intervention to the

TABLE 1
Baseline Characteristics and PET Data of 64 Patients

Patient characteristics	AMI				OMI			
	All AMI	% FDG ≥ NH ₃ (group 1)	% FDG < %NH ₃ (group 2)	<i>P</i>	All OMI	% FDG > NH ₃ (group 3)	% FDG < %NH ₃ (group 4)	<i>P</i>
n	35	16	19		29	16	13	
Age (y)	64 ± 10	65 ± 10	63 ± 10	ns	65 ± 6	64 ± 10	65 ± 7	ns
Sex (male/female)	29/6	13/3	16/3	ns	25/4	15/1	10/3	ns
Location of infarction (anterior/inferior)	17/18	7/9	10/9	ns	21/8	11/5	10/3	ns
Diabetes mellitus	3	3	0	ns	10*	8	2	ns
Peak CK (IU/L)	2885 ± 2581	3177 ± 3248	2613 ± 1848	ns	3876 ± 1769	2489 ± 1613	4742 ± 1284	ns
Stenosis of infarct-related artery (%)	63 ± 33	69 ± 34	58 ± 33	ns	74 ± 30	79 ± 28	68 ± 33	ns
Collateral flow to infarct-related artery (absent/present)	27/8	12/4	15/4	ns	14/15*	6/10	8/5	ns
Angioplasty of infarct-related artery	11	5	6	ns	9	4	5	ns
No. of diseased vessels								
Single-vessel disease	21	13	8	<0.02	10*	6	4	ns
Multivessel disease	14	3	11		19	10	9	
Two-vessel disease	10	2	8		13	7	6	
Three-vessel disease	4	1	3		6	3	3	
Left ventricular ejection fraction (%)	49 ± 12	49 ± 15	48 ± 9	ns	40 ± 14*	43 ± 14	37 ± 13	ns
PET study								
%NH ₃	48 ± 13	46 ± 12	50 ± 13	ns	46 ± 14	47 ± 15	46 ± 14	ns
%FDG	46 ± 13	55 ± 10	39 ± 10	<0.003	48 ± 16	55 ± 15	39 ± 13	<0.02
Marked reverse flow–metabolism mismatch pattern	10				2*			

* $P < 0.05$ vs. all AMI.

AMI = acute myocardial infarction; OMI = old myocardial infarction; FDG = ¹⁸F-fluorodeoxyglucose; NH₃ = ¹³N-ammonia; ns = not significant; CK = creatine kinase.

TABLE 2
Comparison Between Single-Vessel Disease and Multivessel Disease

	AMI		OMI		P
	Single-vessel disease (group AS)	Multivessel disease (group AM)	Single-vessel disease (group OS)	Multivessel disease (group OM)	
n	21	14	10	19	
%NH3	48 ± 12	50 ± 14	50 ± 16	44 ± 13	ns
%FDG	50 ± 11	40 ± 13*	55 ± 18	44 ± 14	ns

*P < 0.05 versus %NH3.

AMI = acute myocardial infarction; OMI = old myocardial infarction; NH3 = ¹³N-ammonia; FDG = fluorodeoxyglucose.

infarct-related artery, number of diseased vessels or left ventricular ejection fraction between groups 3 and 4. There was no significant difference in %NH3 between groups 3 and 4, whereas %FDG was smaller in group 4 than in group 3 (P < 0.02).

Reverse Flow–Metabolism Mismatch and Number of Diseased Vessels

As shown in Table 2, there were no significant differences in %NH3 or %FDG among patients with AMI and single-vessel disease (group AS), with AMI and multivessel disease (group AM), with OMI and single-vessel disease (group OS) and with OMI and multivessel disease (group OM). In group AM, %FDG was significantly smaller than %NH3 (P < 0.05), but there were no significant differences between %NH3 and %FDG in other groups.

As shown in Figure 2, the difference between %NH3 and %FDG (%FDG - %NH3) was significantly smaller in group AM than in groups AS and OS. As shown in Figure 3, the %FDG-to-%NH3 ratio was significantly smaller in

group AM than in group AS. Representative cases are shown in Figure 4.

DISCUSSION

Hospitalized survivors of AMI with multivessel disease have an increased risk of late mortality (17,18). After AMI, patients can be risk stratified using prognostic indicators from stress testing in combination with radionuclide myocardial perfusion imaging (19). Findings have demonstrated the usefulness of exercise testing in the noninvasive identification of multivessel disease (18,20). However, results of predischarge submaximal exercise testing in patients with AMI may contribute to a poor predictive value for multivessel disease (21). In this study, we demonstrated that an FDG defect that was of greater severity than the corresponding NH3 defect, i.e., reverse flow–metabolism mismatch phenomenon, was closely related to multivessel disease in the subacute phase of myocardial infarction, but not in the chronic phase.

In the report by Maes et al. (22) on myocardial flow, metabolism and function in patients with AMI after successful thrombolysis, 13 of 30 patients showed less normalized uptake of FDG than of NH3 at 5 d after infarction. The incidence of reverse flow–metabolism mismatch in their report was comparable with our results. However, their patients who demonstrated less normalized uptake of FDG than of NH3 were included in a group without the perfusion-metabolism mismatch, and the significance of this phenomenon was not discussed. Sawada et al. (23) reported that only 1 of 192 dysfunctional myocardial segments in patients with coronary artery disease had normal perfusion and mildly reduced FDG uptake, but the significance of this segment was not interpreted. Bonow et al. (24) reported that 12 of 98 segments demonstrating mild to moderate (50%–84% of peak activity) irreversible ²⁰¹Tl defect in exercise-redistribu-

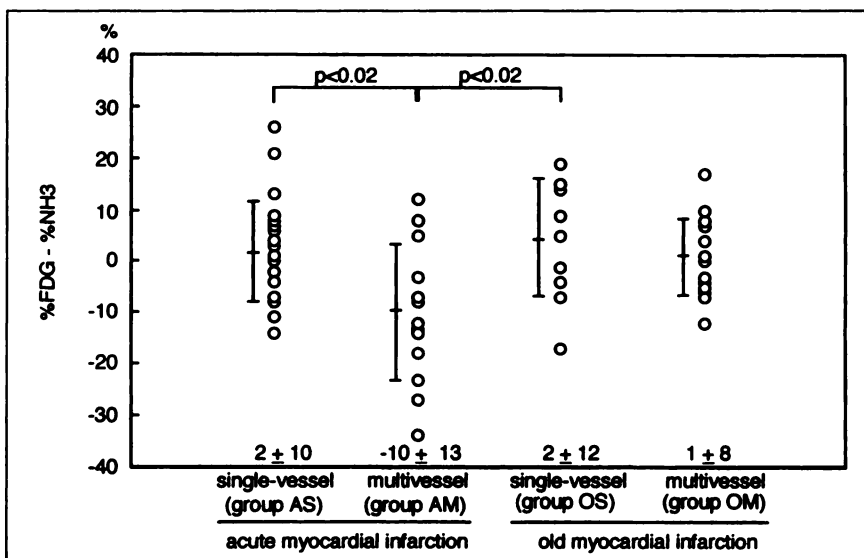


FIGURE 2. Difference between %NH3 and %FDG (%FDG - %NH3) of patients with single-vessel disease and multivessel disease. Difference was significantly smaller in patients with AMI and multivessel disease (group AM) than in patients with AMI and single-vessel disease (group AS), or in patients with OMI and single-vessel disease (group OS).

FIGURE 3. Ratio of %FDG to %NH₃ in patients with single-vessel disease and multivessel disease. Ratio was significantly smaller in patients with AMI and multivessel disease (group AM) than in patients with AMI and single-vessel disease (group AS).

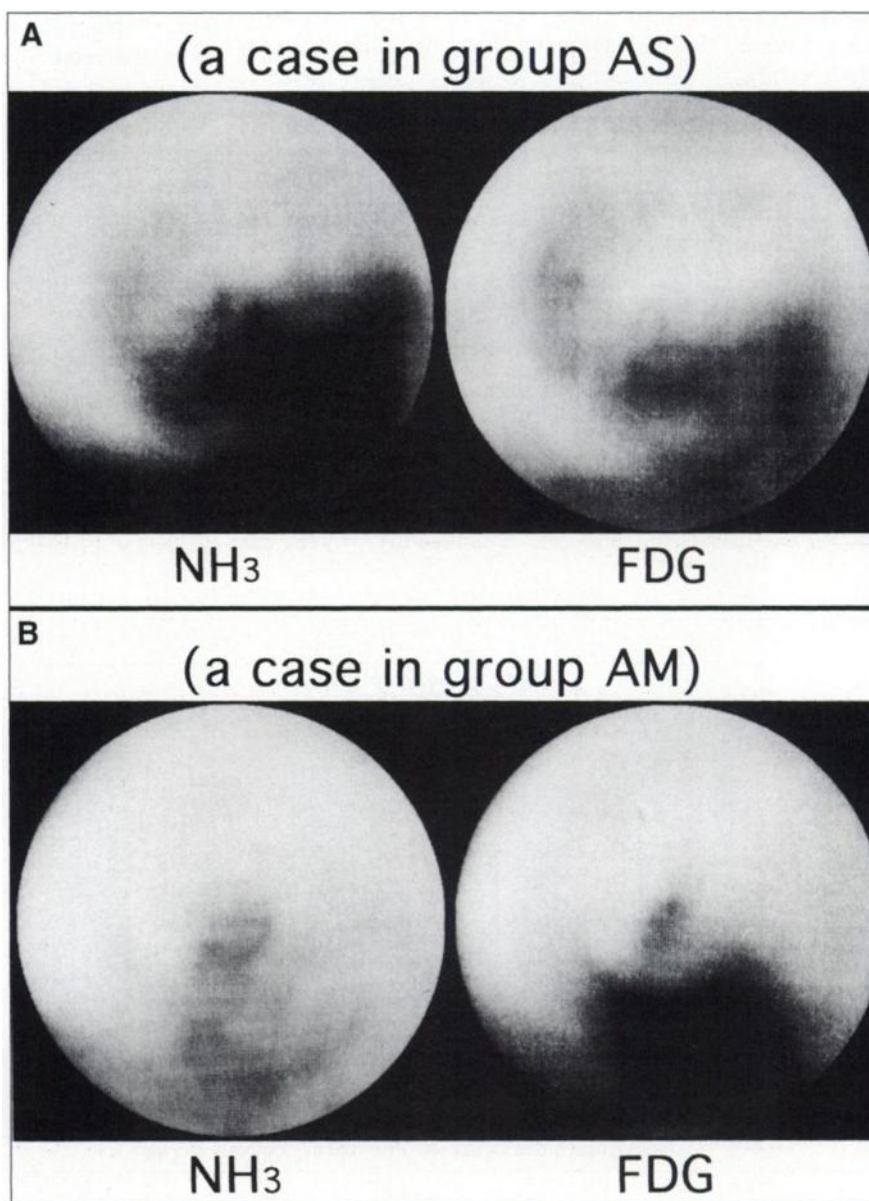
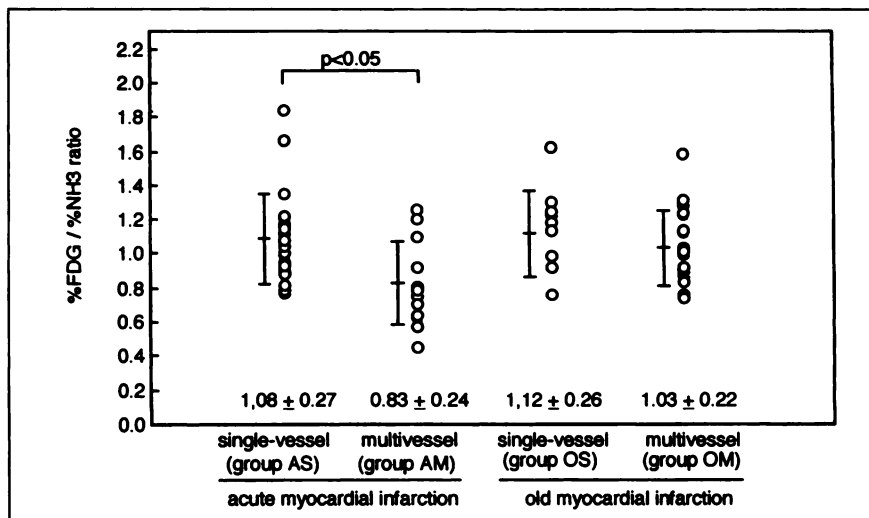


FIGURE 4. Representative bull's eye polar maps. (A) Images from patient with inferolateral wall AMI and single-vessel disease (group AS). In inferolateral segments, NH₃ uptake was severely reduced, and FDG uptake was moderately reduced. Patient showed flow-metabolism mismatch pattern. Coronary arteriography revealed 100% stenosis of right coronary artery. (B) Images from patient with inferior wall AMI and three-vessel disease (group AM). In inferior segments, NH₃ uptake was moderately reduced, and FDG uptake was severely reduced. This patient showed reverse flow-metabolism mismatch pattern. Coronary arteriography revealed 100% stenosis of right coronary artery, 62% stenosis of left anterior descending artery and 68% stenosis of left circumflex artery.

tion ^{201}Tl scintigraphy in patients with chronic coronary artery disease and left ventricular dysfunction exhibited no FDG uptake (<50% of normal reference activity) under glucose loading. The authors considered these segments to represent viable myocardium but did not describe the mechanism of this phenomenon. Grandin et al. (25) identified absolute myocardial blood flow and normalized glucose extraction, but not the normalized FDG-to-normalized NH₃ ratio, as the most powerful predictors of the return of contractile function after coronary revascularization in patients with ischemic anterior wall dysfunction. Of the 25 patients in the study by Grandin et al., 3 demonstrated a normalized FDG-to-normalized NH₃ ratio < 1.0 and had single-vessel disease. These findings indicated a low incidence of reverse flow–metabolism mismatch in patients with chronic coronary artery disease, comparable with our results.

Perrone-Filardi et al. (26) reported that regions with moderately reduced FDG uptake with normal flow occurred commonly in patients with ischemic left ventricular dysfunction and that the majority of these segments showed impaired systolic function at rest and exercise-induced thallium abnormalities that were only partially reversible. The authors suggested that such regions represented an admixture of fibrotic and reversible ischemic myocardium. We investigated NH₃ and FDG uptake in the center of infarction and observed reverse flow–metabolism mismatch in the infarcted territory. Although the infarcted regions showing reverse flow–metabolism mismatch phenomenon were sure to contain infarcted myocardium, we did not investigate whether such regions contained viable myocardium.

Myocardial blood flow is reduced at rest in regions supplied by vessels with >70% area stenosis (27), and coronary sinus adenosine is increased in patients with coronary artery stenosis >70% diameter stenosis (28). Because local myocardial ischemia is associated with release of endogenous adenosine, a sensitive indicator of ischemia (29), myocardium without infarction perfused by a stenotic coronary artery might be exposed to chronic ischemia, resulting in increased glucose uptake (4).

After myocardial infarction, there is a severe vasodilator abnormality, involving not only resistance vessels in infarcted myocardium but also those in myocardium perfused by normal coronary vessels (30). Beyersdorf et al. (31) determined myocardial blood flow and glucose-6-phosphate content in canine models of myocardial infarction simulating single-vessel and multivessel disease. In their study, hypocontractility, unchanged myocardial blood flow and a pronounced increase in glucose-6-phosphate content of remote muscle were observed in dogs with multivessel disease, whereas compensatory hypercontractility, increased myocardial blood flow and a mild increase in glucose-6-phosphate content of remote muscle were observed in dogs with single-vessel disease. The decrease of NH₃ uptake or the increase of FDG uptake in remote myocardium in

patients with AMI and multivessel disease could cause a relative increase of NH₃ uptake or a relative decrease of FDG uptake in infarcted myocardium, resulting in a reverse flow–metabolism mismatch pattern on PET images.

Study Limitations

The major limitation of this study was the small population, which included patients with a history of coronary interventions of the infarct-related artery. Postintervention hyperemia may affect the results in this study. However, the incidence of coronary angioplasty was low and there was no difference in the incidence of angioplasty among the groups. Accordingly, we believe that coronary intervention did not affect our conclusions. However, to confirm these results, studies should be performed in a large population of patients who have undergone conservative treatment.

Diabetes mellitus is a coronary risk factor, and impaired insulin release and insulin resistance affect glucose uptake in myocardium after glucose loading. In this study, 13 patients had diabetes mellitus. However, the incidence of diabetes mellitus was low, and there was no difference in the incidence of diabetes mellitus between patients with single-vessel disease and with multivessel disease in this study. Accordingly, we believe that diabetes mellitus did not affect the conclusions in this study. Moreover, the diabetic population in this study was too small to investigate whether diabetic patients had different results from the nondiabetic patients. It must be determined whether the results of this study are applicable to diabetic patients.

The estimation of relative uptake of tracers on PET images is simple and widely used. However, quantification and observation of serial changes in blood flow and glucose uptake in the myocardium are required to determine the significance and mechanism of the reverse flow–metabolism mismatch phenomenon. The quantification of NH₃ would make clear whether the myocardial blood flow was increased in infarct areas or decreased in remote areas, and the quantification of FDG would make clear whether the myocardial glucose uptake was decreased in infarct areas or increased in remote areas in group AM patients.

In this study, the relationship between flow and metabolism was divided into only two categories, %FDG > %NH₃ and %FDG < %NH₃. As a matter of course, patients should be divided into three categories, a flow-metabolism match pattern, a flow-metabolism mismatch pattern and a reverse flow–metabolism mismatch pattern. The cutoff level of significant difference between %NH₃ and %FDG should be determined by additional investigations. Analysis of the reverse mismatch phenomenon on PET can be performed even in the acute or the subacute phase of myocardial infarction under resting conditions and is very simple. The method described herein may thus be useful for the detection of multivessel disease.

CONCLUSION

The significance of the finding of an FDG defect that was of greater severity than the corresponding NH₃ defect, i.e.,

reverse flow–metabolism mismatch, on PET in patients with myocardial infarction was examined. Results demonstrated that this phenomenon was observed more frequently in patients with AMI than in those with OMI and was related to multivessel disease in patients with AMI. PET studies with glucose loading condition thus yield information about the number of diseased vessels in patients with AMI.

REFERENCES

- Randle P, Garland P, Hales C, Newsholme E. The glucose fatty acid cycle: its role in insulin sensitivity and the metabolic disturbances of diabetes mellitus. *Lancet*. 1963;1:785–789.
- Taegtmeyer H. Energy metabolism of the heart: from basic concepts to clinical applications. *Curr Probl Cardiol*. 1994;19:62–113.
- Liedtke J. Alterations of carbohydrate and lipid metabolism in the acutely ischemic heart. *Prog Cardiovasc Dis*. 1981;23:321–336.
- Opie LH. Hypothesis: glycolytic rates control cell viability in ischemia. *J Appl Cardiol*. 1988;3:407–414.
- Marshall RC, Tillisch JH, Phelps ME, et al. Identification and differentiation of resting myocardial ischemia and infarction in man with positron computed tomography. ^{18}F -labeled fluorodeoxyglucose and ^{13}N ammonia. *Circulation*. 1983;67:766–778.
- Tillisch J, Brunken R, Marshall R, et al. Reversibility of cardiac wall-motion abnormalities predicted by positron tomography. *N Engl J Med*. 1986;314:884–888.
- Tamaki N, Yonekura Y, Yamashita K, et al. Positron emission tomography using fluorine-18 deoxyglucose in evaluating of coronary artery bypass grafting. *Am J Cardiol*. 1989;64:860–865.
- Marwick TH, MacIntyre WJ, Lafont A, Nemecek JJ, Salcedo EE. Metabolic responses of hibernating and infarcted myocardium to revascularization. A follow-up study of regional perfusion, function, and metabolism. *Circulation*. 1992;85:1347–1353.
- Gropler RJ, Geltman EM, Sampathkumaran K, et al. Functional recovery after revascularization for chronic coronary artery disease is dependent on maintenance of oxidative metabolism. *J Am Coll Cardiol*. 1992;20:569–577.
- Gropler RJ, Geltman EM, Sampathkumaran K, et al. Comparison of carbon-11-acetate with fluorine-18-fluorodeoxyglucose for delineating viable myocardium by positron emission tomography. *J Am Coll Cardiol*. 1993;22:1587–1597.
- Schwaiger M, Brunken R, Grover-McKay M, et al. Regional myocardial metabolism in patients with acute myocardial infarction assessed by positron emission tomography. *J Am Coll Cardiol*. 1986;8:800–808.
- Piérard LA, De Landsheere CM, Berthe C, Rigo P, Kulbertus HE. Identification of viable myocardium by echocardiography during dobutamine infusion in patients with myocardial infarction after thrombolytic therapy: comparison with positron emission tomography. *J Am Coll Cardiol*. 1990;15:1021–1031.
- Gropler RJ, Seigel BA, Sampathkumaran KS, et al. The dependence of recovery of contractile function on maintenance of oxidative metabolism after myocardial infarction. *J Am Coll Cardiol*. 1992;19:989–997.
- Mulholland GK, Kilbourn MR, Moskwa JJ. Direct simultaneous production of ^{15}O water and ^{13}N ammonia or ^{18}F fluoride ion by 26 MeV proton irradiation of a double chamber water target. *Appl Radiat Isot*. 1990;41:1193–1199.
- Hamacher K, Coenen HH, Stocklin G. Efficient stereospecific synthesis of no-carrier-added 2- ^{18}F -fluoro-2-deoxy-D-glucose using aminopolyether supported nucleophilic substitution. *J Nucl Med*. 1986;27:235–238.
- American Heart Association Committee Report. A reporting system on patients evaluated for coronary artery disease. *Circulation*. 1975;51:7–12.
- Taylor GJ, Humphries JO, Mellitus ED, et al. Predictors of clinical course, coronary anatomy and left ventricular function after recovery from acute myocardial infarction. *Circulation*. 1980;62:960–970.
- Abraham RD, Freedman SM, Dunn RF, et al. Prediction of multivessel coronary artery disease and prognosis early after acute myocardial infarction by exercise electrocardiography and thallium-201 myocardial perfusion scanning. *Am J Cardiol*. 1986;58:423–427.
- Verani MS. Exercise and pharmacologic stress testing for prognosis after acute myocardial infarction. *J Nucl Med*. 1994;35:716–720.
- Gibbons RJ, Flyke FE III, Clements IP, Lapeyre AC III, Zinsmeister AR, Brown ML. Noninvasive identification of severe coronary artery disease using exercise radionuclide angiography. *J Am Coll Cardiol*. 1988;11:28–34.
- Zhu W, Gibbons RJ, Bailey KR, Gersh BJ. Predischarge exercise radionuclide angiography in predicting multivessel coronary artery disease and subsequent cardiac events after thrombolytic therapy for acute myocardial infarction. *Am J Cardiol*. 1994;74:554–559.
- Maes A, Van de Werf F, Nuyts J, Bormans G, Desmet W, Mortelmans L. Impaired myocardial tissue perfusion early after successful thrombolysis. Impact on myocardial flow, metabolism, and function at late follow-up. *Circulation*. 1995;92:2072–2078.
- Sawada S, Elsnor G, Segar DS, et al. Evaluation of patterns of perfusion and metabolism in dobutamine-responsive myocardium. *J Am Coll Cardiol*. 1997;29:55–61.
- Bonow RO, Dilsizian V, Cuocolo A, Bacharach SL. Identification of viable myocardium in patients with chronic coronary artery disease and left ventricular dysfunction. Comparison of thallium scintigraphy with reinjection and PET imaging with ^{18}F -fluorodeoxyglucose. *Circulation*. 1991;83:26–37.
- Grandin C, Wijns W, Melin JA, et al. Delineation of myocardial viability with PET. *J Nucl Med*. 1995;36:1543–1552.
- Perrone-Filardi P, Bacharach SL, Dilsizian V, et al. Clinical significance of reduced regional myocardial glucose uptake in regions with normal blood flow in patients with chronic coronary artery disease. *J Am Coll Cardiol*. 1994;23:608–616.
- Di Carli M, Czernin J, Hoh CK, et al. Relation among stenosis severity, myocardial blood flow, and flow reserve in patients with coronary artery disease. *Circulation*. 1995;91:1944–1951.
- McLaughlin DP, Beller GA, Linden J, et al. Hemodynamic and metabolic correlates of dipyridamole-induced myocardial thallium-201 perfusion abnormalities in multivessel coronary artery disease. *Am J Cardiol*. 1994;74:1159–1164.
- Berne RM. Cardiac nucleotides in hypoxia: possible role in regulation of coronary blood flow. *Am J Physiol*. 1963;204:317–322.
- Uren NG, Crane T, Lefroy DC, DeSilva R, Davies GJ, Maseri A. Reduced coronary vasodilator function in infarcted and normal myocardium after myocardial infarction. *N Engl J Med*. 1994;331:222–227.
- Beyersdorf F, Acar C, Buckberg GD, et al. Studies on prolonged acute regional ischemia. III. Early natural history of simulated single and multivessel disease with emphasis on remote myocardium. *J Thorac Cardiovasc Surg*. 1989;98:368–380.